CHEMICAL ENGINEERING TRANSACTIONS, Volume 11, 2007
Edited by Sauro Pierucci
 ISBN 978-88-95608-00-6

Oxygen Sensing Properties Of Fe Doped-Srtio$_3$ Powders Obtained By Self-Propagating High-Temperature Synthesis (Shs) And Treated By Ball Milling (Bm)

R. Licheri[a], R. Orrù[a,b*], G. Cao[a,b*], G. Neri[c], A. Bonavita[c], G. Micali[c], G. Rizzo[c]
[a]Dipartimento di Ingegneria Chimica e Materiali, Centro Studi sulle Reazioni Autopropaganti (CESRA), Unità di Ricerca del Consorzio Interuniversitario Nazionale per la Scienza e Tecnologia dei Materiali (INSTM), Università degli Studi di Cagliari, Piazza D'Armi, 09123 Cagliari, Italy
[b]PROMEA Scarl, c/o Dipartimento di Fisica, Cittadella Universitaria di Monserrato, S.S. 554 bivio per Sestu, 09042 Monserrato (CA), Italy
[c]Dipartimento Chimica Industriale e Ingegneria Chimica, Università di Messina, Contrada di Dio, S. Agata, 98166 Messina, Italy

A series of $SrTi_{1-x}Fe_xO_{3-\delta}$ (STO or STFO) powders, with x ranging from 0 to 0.6, were prepared by Self-propagating High-temperature Synthesis (SHS) starting from SrO_2, Ti, TiO_2 and Fe. A ball-milling (BM) treatment was subsequently carried out for further structure refinement and size reduction. Morphological and microstructural characteristics of both untreated and ball-milled SHS samples were investigated by XRD and SEM. Screen-printed $SrTi_{1-x}Fe_xO_{3-\delta}$ SHS powders on alumina substrate were investigated for resistive oxygen sensors operating at high temperature (450-650 °C). STFO powders have shown better performances with respect to the corresponding undoped STO ones. Moreover, when STFO powders were subjected to BM treatment, both temperature-independent resistance characteristics and sensor response greatly improved. On the basis of the reported data, it can be suggested that the ball milling treatment likely acts: *i*) stabilizing the formation of non-equilibrium structures; *ii*) decreasing the particle size, increasing surface defect and hence surface reactivity; *iii*) favouring the substitution of titanium by iron in the $SrTiO_3$ perovskite structure.

1. Introduction

High-temperature oxygen sensors, continuously used in the automotive sector [Gerblinger et al., 1995], convert a chemical signal into an electronic one, which is then relayed to the engine control unit in order to optimize the air-to-fuel ratio (λ), thus reducing deleterious combustion products such as CO, hydrocarbons and NO_x (Foultier, 1982). Recently, metal oxide-based resistive oxygen sensors have attracted much interests as promising alternatives to the conventional amperometric lambda sensors because of their simpler design and manufacturing, with potential cost reduction (Kaiser and Logothesis, 1983). However, for many metal oxide semiconductors the electrical conductivity value, σ, is not only dependent on oxygen partial pressure, P_{O_2}, but is also affected by temperature according to the following equation:

$$\sigma\left(P_{O_2},T\right)\propto P_{O_2}^{1/m}\exp\left(-\frac{E_A}{kT}\right) \quad (1)$$

Thus, to obtain a sensor able to operate in a thermally fluctuating environment (such as the exhaust streams of an automotive engine with temperature ranging from 600 up to 1000 °C under working condition) is necessary to reduce the cross-sensitivity linked to temperature fluctuations. In this contest, particular interest is focused on $SrTiO_3$ (STO), which is stable in a large temperature range due its perovskite crystal structure (Moos et al., 1997). In addition, by properly doping STO with iron, an almost temperature independent resistive material with general composition $Fe_xSrTi_{1-x}O_{3-\delta}$ (STFO) was developed (Williams et al., 1982). Specifically, with $Fe_xSrTi_{1-x}O_{3-\delta}$ powders obtained by conventional solid-state reactions starting from $SrCO_3$, TiO_2 and Fe_2O_3, the best Fe/Ti molar ratio was found around 0.35/0.65 (Moos et al., 1997). In this work, STFO sensing materials are prepared taking advantage of the Self-propagating High-temperature Synthesis (SHS) method (Williams et al., 1982; Moos et al., 1997; Moos et al., 2003). The SHS is a well known synthesis technique based on the occurrence of strongly exothermic reactions that, once ignited, are able to propagate as a self-sustained combustion wave without requiring additional energy (Varma et al., 1998). In the framework of this study, a Ball-Milling (BM) treatment is also subsequently carried out for further structure refinement and size reduction of SHS powders. BM is a solid-state powder process involving welding and fracturing of particles in a high energy ball mill (Suryanarayana, 2001). This technique has been shown to be capable of synthesizing a variety of equilibrium and non equilibrium phase starting from blended elemental or pre-alloyed powders [Suryanarayana, 2001]. Notwithstanding this, the use of BM for gas sensing application has been limited to few cases [Tan et al., 2004; Hu et al., 2004]. Moreover, the influence of iron content on the electrical and oxygen sensing performance of STFO products, obtained by SHS and subsequently subjected to BM, is systematically investigated in this work. To this aim, STFO thick films are deposited by screen printing on interdigited alumina substrates and examined in detail.

2. Experimental materials and methods

The starting mixture to be processed by SHS for the preparation of $SrTi_{1-x}Fe_xO_{3-\delta}$ products were obtained by mixing reactants according to the following reactions:

$2SrO_2+Ti+TiO_2 \rightarrow 2SrTiO_3$ (2)

$2SrO_2+(1-2x)Ti+TiO_2+2xFe \rightarrow 2SrTi_{(1-x)}Fe_xO_3$ (x = 0.35; 0.5) (3)

$SrO_2+0.4TiO_2+0.6Fe \rightarrow SrTi_{0.4}Fe_{0.6}O_{2.8}$ (4)

The amount of Fe in the starting mixture was varied in the range 0-18 wt.%, in order to obtain different Fe-doped strontium titanate powders. Samples code and compositions investigated are indicated in Table 1. Characteristics and sources of reactants as well as details on the experimental procedure and SHS set-up used in this work are described elsewhere for the sake of brevity (Cincotti et al., 2003; Neri et al., 2006).

The SHS products to be used for screen-printing deposition were also further mechanically treated at different milling times (0 – 15 h). Thick films of STO and STFO powders were screen printed on alumina substrates, supplied with comb-like electrodes and a Pt heater, thus preparing oxygen sensor devices. Subsequently, the

devices were treated at 650 °C in air for 2 h to stabilise film texture and microstructure. Sensing tests were accomplished by using a computer-assisted measurement apparatus, measuring the resistance values of the sensors maintained under dry flow of nitrogen and pulsing different concentration of oxygen.

Table 1. Samples ID and compositions investigated

Sample code	$\frac{Fe}{(Fe + Ti)}$ **molar ratio (x)**	**Composition ($SrTi_{1-x}Fe_xO_{3-\delta}$)**
STO	0	$SrTiO_3$
STFO35	0.35	$SrTi_{0.65}Fe_{0.35}O_3$
STFO50	0.5	$SrTi_{0.5}Fe_{0.5}O_3$
STFO60	0.6	$SrTi_{0.4}Fe_{0.6}O_{2.8}$

3. Results and discussions

3.1. Nanopowders preparation and characterization

$SrTi_{1-x}Fe_xO_{3-\delta}$ powders have been prepared by SHS, according to the chemical reactions (2)-(4). All systems investigated displayed a self-sustaining character. This feature is justified by the high exothermicity of the corresponding synthesis reactions. For instance, enthalpy of the reaction (2), used for the synthesis of STO, is ΔH_r^o = - 569 kJ/mol (Barin, 1993). The maximum combustion temperature recorded through a pyrometer during the synthesis of STO was about 2700°C. A drastic reduction of maximum temperature was observed as iron content in the product increases. This outcome is a direct consequence of the corresponding decreased exothermicity. When examining combustion wave velocity, it was generally found that the reaction front propagates slightly slower as iron content in the STFO system is augmented. For instance, front velocity is found equal to 8 ± 0.5 mm/s and 7.3 ± 0.7 mm/s when x=0.35 and 0.5, respectively. The diffraction pattern of the STO product obtained by SHS along with that of the starting mixture are reported in Figure 1. Phase analysis of diffraction patterns showed that reaction (2) proceeds to completion with the formation of cubic $SrTiO_3$. Analogous XRD patterns are also obtained when considering reactions (2) and (3), as reported in Figure 2, where the compositions of STFO products (x=0.35, 0.5, 0.6) are compared with that of STO. However, the XRD patterns of Fe-doped samples show that peaks are shifted toward higher diffraction angles as the iron content increases (see insert in Figure 2). These results are in agreement with previous works reporting that $SrTi_{1-x}Fe_xO_{3-\delta}$ crystallizes in a cubic perovskite structure, with lattice parameters decreasing slightly with increasing iron content (Brinxer et al, 1968). This indicates that $SrTi_{1-x}Fe_xO_{3-\delta}$ solid solutions were formed in the corresponding c-$SrTiO_3$-type structure where Ti(IV) is substituted by Fe(III). After BM, powders show diffraction patterns characterized by remarkable peaks broadening, indicating a refinement of the crystal structure and the increase of the lattice strain with milling time. Specifically, during the early stage of milling, crystallite size refinement occurs significantly within 5 h BM (down to 40 nm), while slows down afterwards, thus reaching a final value in the range

15-20 nm, when BM time is equal to 15 h. This behaviour is consistent with general models for grain size refinement during ball milling proposed in the literature [Suryananrayana, 2001].

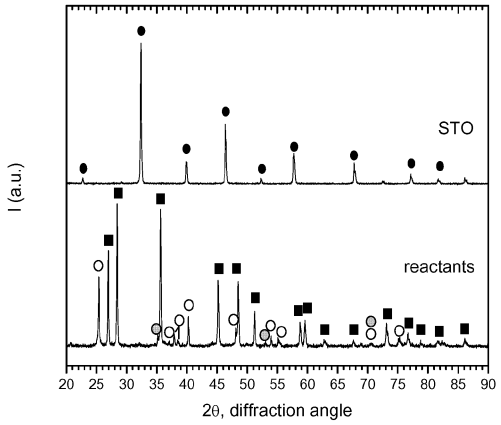

Figure 1. XRD patterns of starting reactants and SHS product STO: ●, $SrTiO_3$; ●, Ti; o,TiO_2; ■, SrO_2.

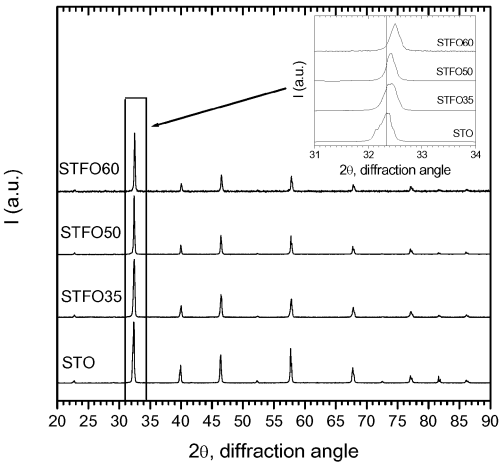

Figure 2. XRD patterns of STO and STFO for different contents of iron as dopant.

3.2. Electrical measurements

The effect of the Fe-doping and ball-milling treatment on the electrical behaviour of $SrTi_{1-x}Fe_xO_{3-\delta}$ powders synthesized by SHS have been investigated in detail, in order to acquire useful information for their possible application in high-temperature oxygen sensors. Figure 3 compares the resistance in air of SHS powders, both un-milled and milled for 5 h. The STO sample shows a high electrical resistance, slightly modified when subjected to ball milling. On the contrary, the addition of iron, coupled with a ball-milling treatment, greatly decreases the electrical resistance. The values of activation energy E_A (cf. Eq. (1)), calculated in the range of temperature investigated (450–650 °C) for 5 h ball-milled SHS powders, are reported in Figure 4 as a function of the [Fe/(Fe+Ti)] molar ratio (x). It can be noted that, increasing the Fe content, E_A decreases correspondingly. In particular, the temperature-independent resistivity (TCR = 0) of the STFO60 sensor can be attributed to the fact that the temperature-dependence of the hole concentration is exactly balanced by that of the hole mobility. This is in agreement with data reported in the literature on differently prepared $SrTi_{1-x}Fe_xO_{3-\delta}$ materials, indicating that TCR reaches a zero value in the range of 0.35-0.65 mole % of iron loading (Moos et al., 1997).

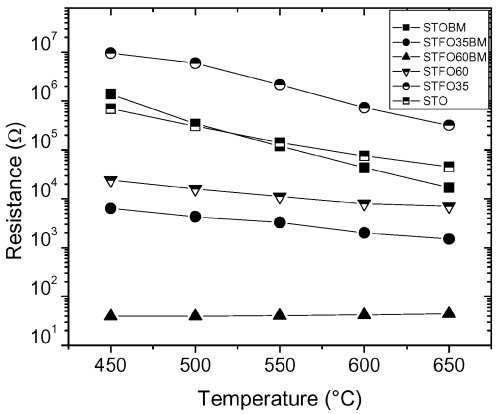

Figure 3. Electrical resistance in air as a function of the temperature of untreated and 5 h ball-milled samples.

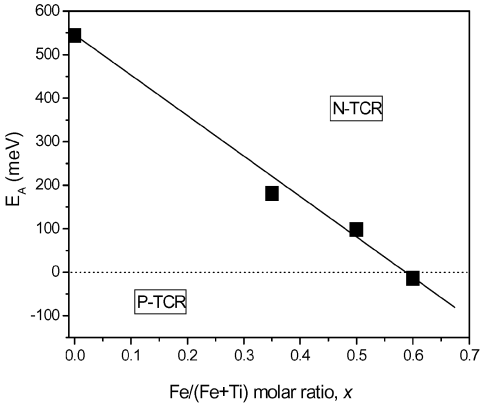

Figure 4. Activation energy, E_A, as a function of the composition of STFO sensors.

3.3. Oxygen sensing tests

Oxygen sensing tests were carried out to investigate the effect of Fe and BM on STFO behaviour to oxygen concentration variation at high temperature. Figure 5 reports the transient response of the STFO60 at 650 °C for different O_2 concentrations. A well reversible behaviour was noted. The relative resistance R_{N_2}/R_{O_2} is used here to express the sensor response, where R_{N_2} is the baseline resistance of the sensor in nitrogen and R_{O_2} is the resistance of the sensor at different concentrations of oxygen diluted by nitrogen (cf. Figure 6). Preliminary experiments have shown that ball milling has a little effect on the response of the STO sensor. However, as seen in Figure 6, for the Fe-doped sensors, the response increases markedly after 0.5 h of ball milling treatment.

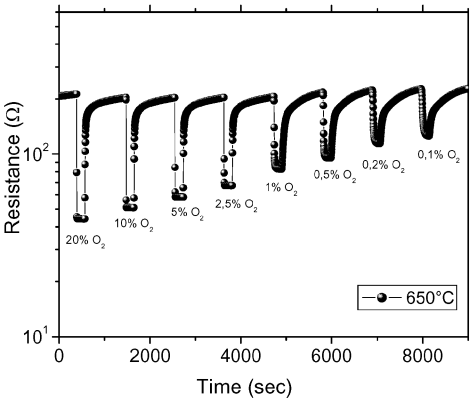

Figure 5. Transient response of the STFO60 ball milled sensor to different O_2 concentrations.

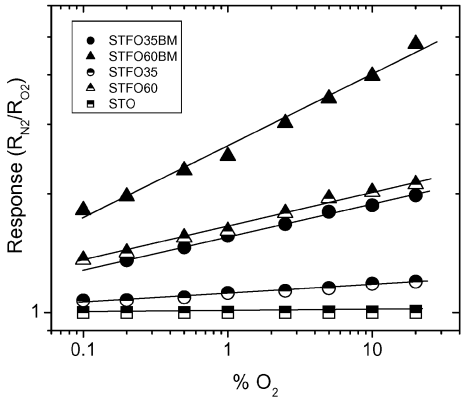

Figure 6. Sensor response to different O_2 concentration of untreated and 5h BM samples. T = 650 °C

The better performances of the ball milled Fe-doped sensors as compared to the untreated ones should be attributed to the structure refinement induced by BM, which allows more titanium substitution by iron.
Summing up, it may be said that both Fe doping and BM contribute to strongly affect the material electrical resistance. Moreover, sensing tests indicate that these factors also cooperate to increase sensor response to O_2 at high temperature. The nanosized particles formed after BM treatment have large surface area and hence, also considering the increase in surface defect, the surface reactivity increases. In addition, bench tests carried out under simulated engines conditions have confirmed these good characteristics, showing the negligible interference on the sensor response of high concentrations of CO_2, NO_X and HC. The obtained results indicate that resistive oxygen sensors based on nanopowders of STFO are promising candidate as λ-probes for lean-burns engines.

4. Conclusions

In this work, $SrTi_{1-x}Fe_xO_{3-\delta}$ (STFO) powders with different Fe content were synthesised by SHS. Results have shown that the SHS technique coupled with high-energy BM is a very effective route to prepare nano-structured solid solutions for oxygen-sensing applications. The effects of the iron content and ball-milling treatment of the $SrTi_{1-x}Fe_xO_{3-\delta}$ (STFO) powders on the electrical characteristics and response to oxygen at high temperatures have been examined in detail. Ball-milled STFO60 thick films have shown the better performances in terms of temperature resistance independence as well as sensor response.

5. References

Barin, I., Thermochemical data of pure substances, VHC (1993).
Brixner, L.H.,1968, Mat. Res. Bull. 3, 299.
Cincotti, A., R. Licheri, A. M. Locci, R. Orrù and G. Cao, 2003, J. Chem. Techn. Biotech., 78, 122.
Fouletier, J., 1982, Sens. Actuators, 3, 295–314.
Gerblinger, J., K.H. Hardtl, H. Meixner, R.Aigner, W. Gopel (Ed), 1995, Sensors, A Comprensive Survey, 8, Weinheim, 181.
Hu, Y., O. K. Tan, W. Cao, W. Zhu, 2004, Ceramics International, 30, 1819.
Kaiser, W:J., E.M. Logothetis, , 1983, SAE Paper 830167.
Moos, R., W. Menesklou, H.-J. Schreiner, K.H. Hardtl, 1997, US Patent 6,319,429.
Moos, R., F. Rettig, A. Hurland, C. Plog, 2003, Sens. and Actuators B, 93, 43.
Neri, G., Bonavita, A., Micali, G., Rizzo, G., Licheri, R., Orrù, R., Cao, G., 2006, Sens. Actuators B, , doi: 10.1016/J.snb.2006.12.008.
Suryanarayana, C., 2001, Prog. Mater. Sci., 46, 1-184.
Tan, O. K., W. Cao, Y. Hu, W. Zhu, 2004, Solid State Ionics, 172, 309.
Varma, A., A.S., Rogachev, A.S., Mukasyan, S., Hwang, 1998, Adv. Chem. Eng., 24, 79.
Williams, D.E., B.C. Tofield, P. McGeehin, 1982, European Patent EP 0062994.